



Current Research Trends of Electrical Arc Machining (EAM) with Reference to Electrical Discharge Machining (EDM)

Ranjeet Singh Thakur¹, Dr. Shrihar Pandey^{2*}, Shiwangi Mishra³, Babli Lodhi⁴, Akash Mishra⁵

¹Research Scholar, Department of Mechanical Engineering, School of Engineering, Eklavya University Damoh-470661, India. Email: rst2203@gmail.com

^{2*}Associate Professor and Head Department of Mechanical Engineering, School of Engineering, Eklavya University Damoh-470661, India. Email: shriharpandey@gmail.com

³Research Scholar, Department of Mechanical Engineering School of Engineering, Eklavya University Damoh-470661, India. Email: shivangi1292@gmail.com

⁴Assistant Professor, Department of Mechanical Engineering, School of Engineering, Eklavya University Damoh-470661, India. Email: Bablilodhi890@gmail.com

⁵Assistant Professor, Department of Mechanical Engineering, School of Engineering, Eklavya University Damoh-470661, India. Email: mishraakash38@gmail.com

***Corresponding Author:** Dr. Shrihar Pandey
Associate Professor and Head

^{*}Department of Mechanical Engineering, School of Engineering, Eklavya University Damoh-470661, India.
Email: shriharpandey@gmail.com

Submission- 16th Sept. 2023 Revision-10th Oct.2023 Accepted- 5th Nov. 2023 Published- Nov. 2023

Abstract

The thermal energy-based unconventional machining technique known as "electrical arc machining" uses arc energy to melt and vaporize work piece material. Advanced materials including metal matrix composites, super alloys, and conductive ceramics may be efficiently machined by electrical arc machining. When it comes to the pace of material removal, the procedure is thought to be more effective than the majority of other non-traditional machining techniques. However, it is constrained since it produces a very subpar surface finish. Other limitations include the rate of tool wear, the formation of recast layers, surface and subsurface cracks, and, to some extent, geometrical accuracy. The research that has been done so far in the area of electrical arc machining is thoroughly analyzed in this work. The article summarizes the thorough practical and theoretical investigations on electrical arc machining that have been carried out in order to elucidate the consequences of various input control parameters on various quality attributes. The study's final section looks at possible directions for future work in electrical arc machining. Additionally, it contains past modeling and optimization research in this area.

Keywords Unconventional Machining Process, Electrical Arc Machining, Electrical Discharge Machining, Material Removal Rate, Tool wear Rate, Inter Electrode Gap, Response Surface Model (RSM) and Artificial Neural Network (ANN), Orthogonal Array (OA)

1. Introduction

Machining remains a crucial manufacturing process for achieving precise size, shape, and surface integrity of workpieces. However, it is just one piece of the larger puzzle in the world of materials science and manufacturing, where continual innovation is necessary to meet the demands of modern technology. Although machining remains a crucial manufacturing process for achieving precise size, shape, and surface integrity of workpieces. However, it is just one piece of the larger puzzle in the world of materials science and manufacturing, where continual innovation is necessary to meet the demands of modern technology. Though effective, the use of traditional machining techniques is occasionally constrained when cutting modern materials. To meet the needs of the modern world, researchers have devised a wide variety of unconventional machining methods (UMPs). [1] UMPs are primarily categorized according to the type of energy they use, such as mechanical, chemical, electrochemical, thermal, etc.

1.1 Electrical dischargemachining

The most popular thermal energy-based UMP today is electrical discharge machining. During EDM, the tool electrode and workpiece electrode are immersed in a dielectric. When the correct voltage is applied between the two electrodes, an electrostatic force develops and the free electrons on the surface of the cathode begin to move in the direction of the anode precisely at the moment when the local gap between the two electrodes is the smallest. As a result of collisions between moving electrons and dielectric molecule

Ionization of the dielectric results in the production of more electrons and positive ions. These positive ions and electrons collide to form more positive ions and electrons. When the number of electrons and ions is extremely high, plasma is formed very quickly. Plasma is a thin column of molecules made of an ionized dielectric fluid. The surface of the anode is struck by fast moving electrons and their kinetic energy is converted into heat, raising the local temperature to 8000-12000°C[2]. The work material melts or evaporates at such a high temperature. Similar to negative ions, when positive ions hit the surface of the cathode, melting and evaporation occur. The molten material is not ejected from the plasma tube due to the high pressure inside. Once the shutdown time begins, the plasma channel collapses and the molten material is ejected by the shock wave and the flowing dielectric².

Input parameters that determine EDM performance include peak current, pulse on time, pulse off time, voltage, inter-electrode gap (IEG), electrode rotation, and workpiece rotation. A schematic of the EDM is shown in Figure 1[2]. The peak current and on-time of the EDM pulse are typically limited to 100 A and 1000 ms³, respectively, according to past studies. Despite being the most commonly used technology in industry, EDM is considered an inefficient process in terms of material removal rate (MRR), tool wear rate (TWR) and specific energy requirements. A thermal energy-based UMP that shares many characteristics with EDM is electric arc machining (EAM). A discussion of EAM is included in the section that follows.

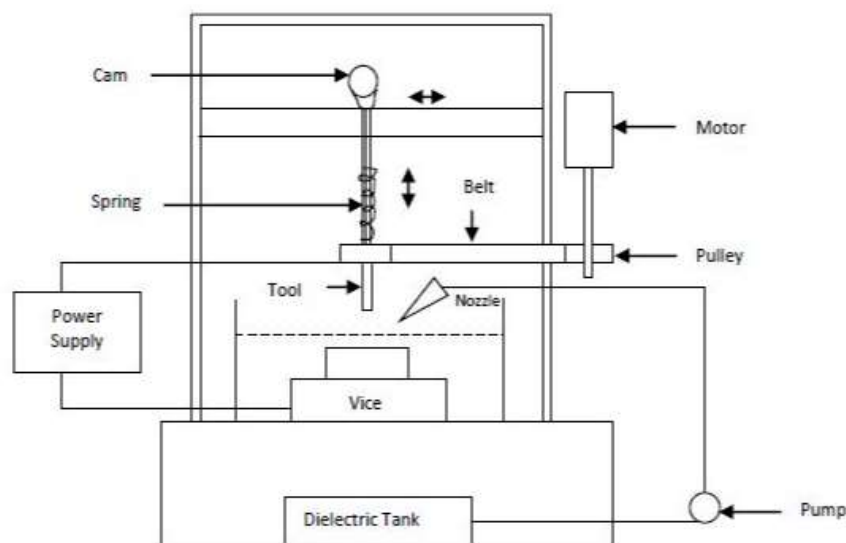


Figure 1: Flowchart for the EDM Process

1.2 Electrical arc machining

EAM components, which are identical to those found in EDM, include the tool electrode and workpiece, feed system, dielectric and dielectric feed system, and feed mechanism. However, EAM can use both direct current and pulsed direct current. Pulsed DC is used in EDM. If pulsed DC is used in the EAM, the pulse turn-on time will be quite long. According to existing research, the EAM pulse lasts for longer than 100 ms. According to the research that is currently accessible, the EAM has been used with pulse durations up to 20,000 ms[4].

1.2.1 Removal of material mechanism

The EAM experiences the same plasma channel creation as the EDM. The basic characteristic of EDM is the volatility of the discharge because the spark's location is constantly shifting. In contrast, EAM is a consistent discharge mechanism with a constant discharge site. The same is caused by the EAM's inadequate deionization of the dielectric. Similar to the EDM, melting and vaporization also serve as the EAM's method for removing material.

However, compared to spark plasma in the EDM, arc plasma in the EAM has a far higher energy density and temperature. As a result, the EAM melts and vaporizes substantially more than the EDM [5]. RMABM and HABM are two examples of commonly used systems for this.

Mechanical motion arc breaking method is another name for the RMABM. Arc plasma is broken in RMABM by using relative motion of the tool and workpiece[4]. In the HABM, the dielectric is fed through tubular or bundled hollow electrode into the machining zone. Dielectric exerts a high hydrodynamic force that elongates, compresses, and splits the plasma channel, preventing stationary arcs. Injection flushing and side flushing are occasionally used in conjunction to boost efficiency [6]. The input control factors and output control factors for the EAM process are shown in Figure 2.

Variation of EAM. EAMs can be categorized based on the type of arc-interruption mechanism, such as RMABM or HABM. According to Figure 3, the literature currently available divides EAM into the following categories.

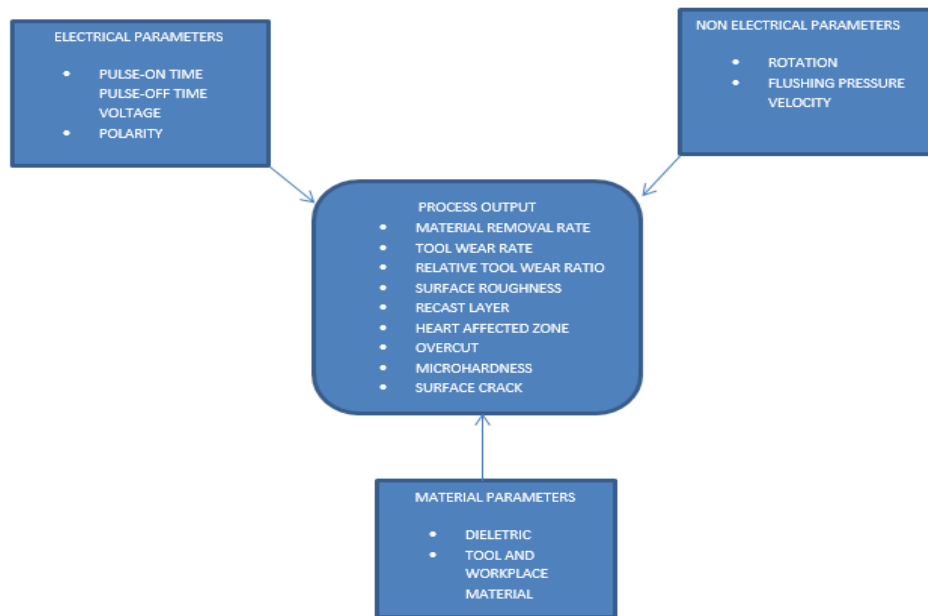


Figure 2: Process Parameter in the EAM

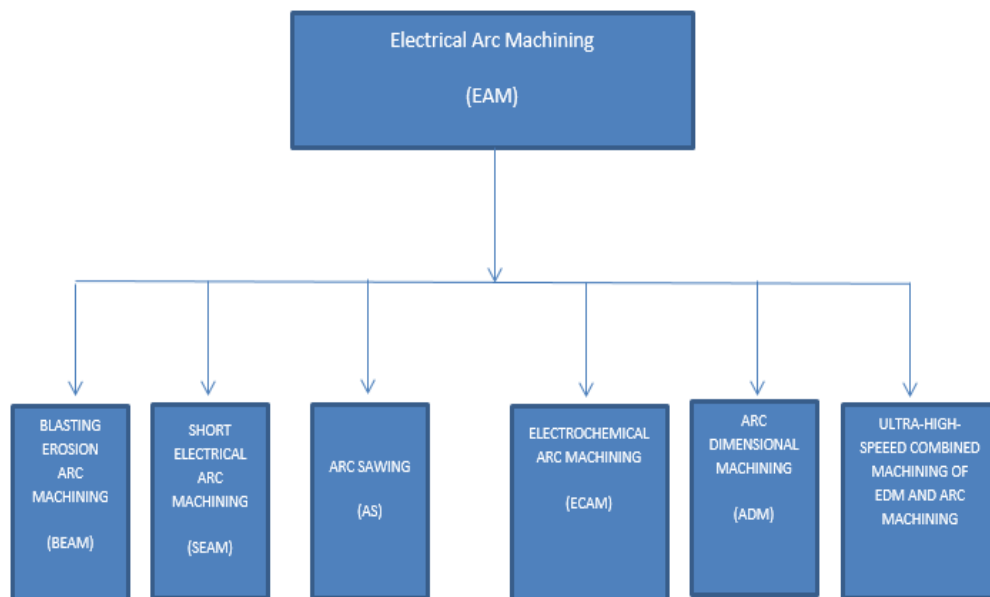


Figure 3: EAM Variants

1.2.2 Dimensional machining in an arc

The arc plasma is stretched or broken by the ADM using the HABM, which uses fluid dynamics. The machining area is enclosed in an airtight enclosure during the process. The dielectric liquid is drawn in by a very thin electrode with a flushing channel. The direct current serves as the power source for machining and the channel is used to wash away the generated impurities. Researchers were able to carve an arc with an MRR of approximately 16,000 mm³/min (for an electrode size of 500 mm² and a current of 1,000 A) during ADM of carbon steel [7]. Arc sawing is essentially an arc cutting technique that slashes through highly conductive materials with low voltage (500 V) and high current (500 A) DC. The working medium is either an electrolyte solution or air. The procedure uses a disc electrode with vanes and air as the working medium. To remove the material melted as a result of the arcing between the workpiece and the disc electrode, these vanes are subjected to moderately pressured air (4-5 bars). The technique is limited by its high noise level and harmful fume production[8,9].

1.2.3 Milling with a brief electric arc

In order to create a steady arc discharge, short electric arc machining (SEAM) uses low voltage (15-42 V) and extremely high current (up to 10,000 A). It uses a high-pressure (3.5-8.5 bar) dielectric made from a certain ratio of air and water. The power source for SEAM can be continuous or pulsed DC. Fluid that has been compressed aids in the efficient ejection of trash. The MRR from the SEAM could be as high as 1.1-105mm³/min[9].

1.2.4 Blasting and Erosion Machining

Arc jet erosion machining (BEAM) is a newer EAM technique that uses the hydrodynamic force of the dielectric to prevent a stationary arc. High-velocity fluid is fed into the machining zone using a bonded hollow cylindrical electrode. An injection mode of fluid delivery is used. The arcing plasma column is bent, elongated or even broken by the enormous hydrodynamic force created by the high-velocity fluid during the BEAM, and the high-powered jet blasts the molten material explosively. BEAMs are divided into two types in all available literature: positive BEAMs and negative BEAMs. The tool electrode is connected to the positive pole of the power source in the case of a positive BEAM and to the negative pole in the case of a negative BEAM.

1.2.5 Cutting with an electrochemical arc

A thermal energy-based UMP called EDM uses spark energy to produce the required shape. The anode and cathode are separated by a dielectric medium in this device. An UMP called electrochemical machining (ECM) removes material using electrolysis. The working medium in the ECM is electrolyte. ECAM is a method that combines the benefits of EDM and ECM. For regulated material removal, arcing or sparking in the electrolyte happens in ECAM[10]. Electrochemical discharge machining, electrochemical spark machining, and spark-assisted chemical etching are names given to it by a small number of researchers.

1.2.6 Combining arc and EDM

Machining at extremely high speeds. UHSEDAM is an acronym for ultra-high-speed combined arc and EDM machining. It combines a pulse generator (high voltage/low current) with a DC (low voltage/high current) power supply. To prevent interference, diodes are used to disconnect the two power sources from one another. The pulse power source, which provides a strong enough electrostatic field, enables the breakdown of the dielectric and the subsequent creation of the plasma channel. As ignition begins and the plasma channel begins to expand, the DC source simultaneously supplies a strong discharge current to the plasma channel. The plasma channel is kept running by the DC power source even during the pulse off interval. In traditional EDM, the plasma channel disappears during the pulse off period and the material is removed. In contrast, the dynamic activity of the dielectric in UHSEDAM breaks the plasma channel and also helps with material removal and workpiece cooling. Figure 4 shows the UHSEDAM schematic.

1.2.7 Application for EAM

All conductive materials, regardless of their hardness, can be machined because it is a process based on thermoelectric energy. The use of EAM to automate many engineering materials such as Ti-6Al-4V alloys, Inconel 718, spring steel, AISI D2 steel and carbon steel in the literature, these include SiC-Al metal matrix composite (MMC). In the early stages of the study, a stainless-steel plate in a Japanese nuclear reactor was successfully cut by EAM. Along with it, radioactive containers were disassembled⁹. Positive results have been obtained when it has been applied to cement grinding roller. The technique has been used to quickly section fragile parts and hardened alloys[12]. As depicted in Figure 5, it has recently been employed to create intricate profiles like gears, impellers, and others.

2. Literature Review

Rate of material removal and rate of tool wear. Weight/volume of material removed per unit of time from the surface of the workpiece or from the surface of the tool, is referred to as material removal rate and tool wear rate. Any machining operation should always aim to increase material removal rate and decrease tool wear rate. The relative electrode wear ratio can also be used to gauge a process' effectiveness in some cases. The REWR ratio measures how much workpiece material is lost to tool material during machining. It goes without saying that businesses and the scientific community want to reduce REWR. How well EAM functions in terms of material removal rate and relative electrode wear rate have been studied by several academics. BEAM on AISI D2 steel was performed by Zhao et al.[13] using bundled graphite electrodes and a water-based dielectric fluid. The parameters selected for the input control were peak current, pulse-on time, pulse-off time, polarity, and fluid flushing pressure. As the peak current and pulse duration grow, they discovered that the MRR constantly climbs for both positive and negative BEAMs. In comparison to the positive BEAM, the MRR for the negative BEAM was over 5.6 times higher. The scientists studied the behavior of REWR and found that the minimal REWR during the negative BEAM is less than 1%, whereas it is about 18% during the positive BEAM. That might be as a result of how the anode and cathode transfer energy differently. Studies show that compared to the cathode, the anode uses a bigger percentage of the energy [5]. It is shown that the MRR increases for both negative and positive BEAMs with an increase in flushing pressure. The same could be attributed to superior gap conditions, such as better debris ejection and improved discharge frequency. Gu et al. [14] implemented positive and negative BEAM using

20 vol% SiC/Al MMC and varied peak current, pulse-on time, and pulse-off time. They discovered the same thing Zhao et al.'s study [13] did, namely that the negative BEAM yields a significantly higher MRR than the positive BEAM. At a peak current of 500 A during the negative BEAM, they attained an MRR of 8276 mm³/min. The greatest and least REWR during milling, according to their experimental findings, are, respectively, 3.10% and 2.02%. Additionally, it is noticed that REWR falls as peak current and pulse-on time rise. The increased discharge energy and energy density brought on by the above machining circumstances may be the cause of the increased MRR and TWR. However, because the MRR rise outweighs the TWR increase, the REWR is ultimately decreased.

Using BEAM on Ti-6Al-4V alloy, **Chen et al. [15]** achieved an MRR of 21,000 mm³/min. They also observed that the MRR increased with peak current and pulse on time, while it decreased with pulse off time. They proposed the use of high peak current, long pulse on time and short pulse off time to improve the machining efficiency in terms of MRR and REWR. They found that the REWR was stable (about 3.1%), regardless of processing conditions. By comparing positive and negative BEAM, they found that positive BEAM leads to lower MRR and higher REWR. Xu et al. [16] evaluated positive and negative BEAM during EAM of nickel-based alloy GH4169. Their experimental findings showed that negative BEAM produces an MRR that is significantly greater than positive BEAM (which can reach a maximum of 3278 mm³/min; up to 14,000 mm³/min). Similarly, the maximum REWR for positive and negative BEAM was found to be 1% and 18.3%, respectively. In another study, Zhao et al. [6] used BEAM to machine Inconel 718 by adjusting the peak current and pulse on time. At a peak current of 600 A, the highest MRR was achieved at 11,300 mm³/min, while the REWR was less than 3%. In order to perform EAM on W18Cr4V tool steel, Zhang et al. [4] varied the flow rate (0–3 L/min) of the dielectric fluid. They concluded that excessive flushing simultaneously reduces MRR and TWR.

Shen et al. [17] evaluated MRR and REWR machining of AISI 304 stainless steel using dry EAM, dry EDM and dry hybrid machining (fused dry EAM and EDM). Peak current, air flow and electrode rotation were used as input control parameters. Compared to dry EDM and dry EAM, they found that the MRR for dry hybrid machining is 100 times greater. Moreover, they observed that MRR increases significantly while REWR decreases with increasing airflow rate. The efficient extrusion of molten material that occurs as the air velocity increases the MRR. Along with the increase in airflow rate, the deposition of molten material on the tool electrode also increases, reducing the REWR. They also observed that as the electrode rotation increases, the MRR increases but the REWR maintains a constant value. The outward flow rate of the fluid increases as the electrode rotation increases, aiding in better impurity expulsion and increasing the MRR. W9Mo3Cr4V high-speed steel was subjected to SEAM according to Zhu et al. [18] using tubular graphite electrodes. The studies were performed using the L9 orthogonal array experiment. They found that as the peak current, spindle speed, and combined pulse voltage increased, the MRR tended to increase, but as the purge pressure increased, the MRR tended to decrease. They concluded that the most significant control element for MRR is the peak current. They found that TWR increases as peak current and spindle speed increase. Peak current and spindle speed were found to be the two most significant factors for TWR. Wang et al. [19] performed UHSEDAM on Ti-6Al-4V titanium alloy. They investigated the effects of electrode polarity, peak voltage, peak current, and internal flushing pressure on MRR and REWR. MRR (1227 mm³/min) with positive polarity is one-third that of negative polarity and REWR is more than twice as high according to experimental data.

In a different study, Inconel 718 superalloy was subjected to the UHSEDAM by **Wang et al. [19]** Peak current and dielectric flushing pressure were employed as input control parameters. Using a peak current of 920 A, they were able to attain the MRR of 15,162 mm³/min and the REWR of 1.725%. Additionally, it was found that the MRR rises as the peak current and injection flushing pressure rise. Peak current had little effect on the REWR, but the flushing pressure rise caused it to drop off quickly. In a different study, **Wang et al. [20]** used a pipe graphite electrode to perform UHSEDAM on AISI H13 steel. It was possible to reach the MRR of 12,786 mm³/min at a peak current of 699 A. On the MRR and the REWR, the effects of peak voltage, flushing pressure, and electrode rotation were examined. They found that while the REWR decreases as peak voltage rises, the impact of voltage on the MRR is minimal. Shock wave that debris causes also contributes to tool wear. IEG rises with increasing voltage. The tool experiences a smaller shock wave with higher IEG, which lowers the REWR. It was found that the MRR increases while the REWR rapidly drops flushing pressure of the injection is raised from 0.021 to 0.092 MPa. Behavior of material removal rate and relative electrode wear rate with respect to electrode rotating speed showed that, initially, both attributes decreased as the rotational speed increased, but around 1200 rpm/min, they began to somewhat fluctuate. Using various electrolytes.

Paul et al. [8] looked at how Inconel 718 superalloy performed during AS. For their experimental investigation, they used electrolytes of sodium silicate, sodium chloride, potassium chloride, and sodium sulfate. According to their research, sodium silicate has a maximum MRR of about 700 mm³/min. Furthermore, it was found that the conductivity of the electrolyte had a significant effect on the MRR. For sodium silicate, MRR increases with increasing conductivity, but for other materials there was no clear pattern of MRR variation with conductivity.

Surface consistency, for better-quality goods, certain surface and subsurface factors represented by surface integrity must be regulated. In thermal energy-based operations (especially in EDM and EAM), the surface finish, RL, HAZ,

micro fractures, oxides/scale growth, and subsequent discharge crater are all components of the SI. One of the key machining goals is to produce a better surface finish. Surface roughness (SR), a measure of surface finish, is used. The surface finish is better the lower the SR. RCL is a layer that develops on the workpiece's surface as a result of the molten material resolidifying. Due to its great hardness and fractures, RCL is not appealing. HAZ is simply the area of the base material where the microstructure and properties have been impacted by intense heat. The quenching by dielectric causes thermal strains during pulse-off time, and these thermal tensions cause fractures to form in the surface or subsurface.

Zhao et al. [13] found that negative BEAM produces an extremely high SR (on the order of 360 mm) when machining AISI D2 steel, while positive BEAM produces a lower SR (on the order of 28 mm). They also observed that as the peak current and pulse duration increase, the SR increases for both positive and negative BEAMs. Additionally, they noticed that improving the flushing pressure improved the surface quality. Gu et al.[14] found that the surface produced by positive BEAM during 20 vol% SiC/Al MMC BEAM is significantly smoother than the surface produced by negative BEAM. However, several microcracks were noted in all cases. Additionally, it was noted that the RCL thickness varied and was thicker in the negative BEAM compared to the positive BEAM, where it was thin and uniform. The BEAM negative surface has a larger range of oxygen and carbon than the BEAM positive surface.

Shen et al. [17] used dry EAM on AISI 304 steel and found that surface gloss increased with air flow rate and electrode rotation. The improvement in surface quality may be due to improved debris ejection, which will increase the randomization of the discharge location. Examination of the surface showed that graphite from the tool electrode had migrated towards the surface of the workpiece. This was proven by the presence of a black spot on the surface. Zhang et al. [4] discovered that surface quality in terms of SR improves when dielectric flow rate is increased during EAM of tool steel. A higher flow rate results in a smaller crater diameter,

which lowers the SR. **Zhu et al. [18]** performed SEAM on W9Mo3Cr4V high-speed steel. They concluded that flushing pressure and peak current are the main regulating parameters of SR. The peak current increases as SR increases and the purge pressure increases as SR decreases. The highest measured SR was 699 mm with a current of 600 A. According to Wang et al. [11], during UHSEDAM of Inconel 718 superalloy, the HAZ is minimal and the RCL thickness at the center of the crater is less than 30 mm. They also observed that the thickness of the remelted layer is not affected by the peak current. There were only a few small cracks on the machined surface according to the SEM surface photograph.

Xu et al.[16] observed that the SR for both positive and negative BEAM increases as the peak current rises when milling nickel-based GH4169 alloy. While it was 3 mm in positive BEAM, the minimum SR obtained in negative BEAM was 274 mm. The positive BEAM produces a surface with much less remelted ripples, attached debris particles and microcracks than the negative BEAM, according to SEM observations. Remelted ripples and debris particles were rarely visible on the positive BEAM machined surface, but were visible on the negative BEAM machined surface. BEAM was applied to Inconel 718 superalloy by **Zhao et al[6]**.The HAZ was found to be less than 200 mm. The use of coated electrodes and a water-based dielectric effectively removes heat from the workpiece, prevents overheating and reduces HAZ. During UHSEDAM steel, **Wang et al. [20]**found many craters and droplets that resembled fish scales.The width of the crater was found to be greater than its depth and the thickness of the upper layer was less than 100 mm. HAZ on a component that has undergone EAM processing is, according to **Paul et al. [8]**, **Zhou et al. [21]** investigated the effects of feed, air pressure, water pressure and relative spindle speed during SEAM of carbon steel. The highest SR and HAZ values recorded were 514 and 340 millimeters. The researchers also concluded that the most and least important process control parameters are air pressure and water pressure.

Thermal and mechanical properties, residual stresses during BEAM SiC/Al MMC were investigated by Gu et al.[14] Their experimental results showed that residual strains are produced by both positive and negative beams. However, compared to the negative BEAM, which produces a maximum residual stress of about 40 MPa, the positive BEAM produces a maximum residual stress of up to 115 MPa. They added that at a depth greater than 0.4 mm from the machined surface, the residual stress is similar to the matrix of the material. Chen et al. [15] reach similar conclusions about the residual stress during BEAM of Ti-6Al-4V alloy. Wang et al.[11] evaluated the microhardness of the surface and subsurface layer by UHSEDAM of Inconel 718 superalloy. They found that the microhardness of the remelted layer was approximately 295 Hv, which was significantly less than the microhardness of the base material (510 Hv) up to a depth of 20 mm from the surface.

Geometric features. The geometrical component includes form flaws including taper, overcut, circularity, and others an arc travelling in the EAM's flushing direction creates a crater with a following track. According to studies, positive BEAM produces smaller craters than negative BEAM [4,12], and as a result, the positive BEAM produces smoother surfaces than the negative BEAM. Conical brass needles were employed by Zhang et al.[4] to perform single-discharge EAM investigations on W18Cr4V steel. The dielectric medium was chosen to be pure water. The polarity and flow rate were shown to have a significant influence on the crater geometry. A higher flow rate causes the crater to become smaller and promotes the growth of the tail. The behavior of the positive and negative polarity in the variation of the

crater diameter with flow rate is comparable. In the UHSEDAM of AISI H13 steel, Wang et al. [20] assessed the impact of electrode rotation on the groove edge. They came to the conclusion that the electrode's rotational speed and direction had an impact on the edge quality and shape

2.1 Modeling and optimization studies

A paradigm model in manufacturing essentially creates the relationship between input control elements and output through a mathematical equation. To forecast the behaviors of complicated processes and to assist save time and money, models are tremendously helpful. The research community generally accepts three different types of models. The three of them are the mechanistic model, analytical model, and empirical model. Since they don't require a thorough understanding of the subject, empirical models are simple to create. But to create the empirical model, much experimental work is needed. Examples of empirical models include response surface model (RSM) and artificial neural network (ANN) model. Experimentation uses design of experiment (DOE) techniques such as factorial design, central composite design, orthogonal array (OA) based on Taguchi method, Box-Behnken design, etc.².

Deep understanding of the procedure, presumptions, and science is necessary for the creation of analytical models. But a wide range of control parameters can be employed with these. The three different categories of analytical models are:

- (i) solution-based numerical
- (ii) solution-based numerical and
- (iii) solution-based stochastic.

The mechanistic model shares some characteristics with both the analytical and empirical models.

Only a small number of academics have investigated modeling and optimization in EAM. Gu et al.[14] developed a linear regression model for MRR and REWR using peak current, pulse and pulse timing as well as positive BEAM Al/SiC MMC. They did not perform a statistical evaluation to determine the adequacy of the models. Chen et al. [15] developed comparable regression models for BEAM Ti-6Al-4V. Peak current, pulse on time and pulse off time were considered as input control parameters. They also performed single-objective constrained optimization on MRR and REWR using the MATLAB toolbox. The MRR and REWR values they obtained through optimization were 20,300 mm³/min and 2.825%, respectively. Xu et al. [15] used positive BEAM on nickel base alloy GH4169 to develop regression models for MRR, REWR and SR and found the models to be reliable. By adjusting the spindle speed, liquid pressure, and gas pressure, Zhou et al.[22] performed SEAM on spring steel. They created a regression equation for SR and concluded that fluid pressure is the most important element.

2.2 Findings of Literature survey

An extensive literature review revealed that EAM can address one of the main problems with UMPs – their lack of effectiveness in terms of low MRR. MRR in EAM has been found to be comparable to conventional machining processes [23]. Another limitation of EDM is TWR. The authors' literature review shows that REWR in EDM ranges from 0.01% to 377%.²⁴⁻³² However, REWR for EAM has been reported to range between 1 and 4 percent. It has occasionally been found to be closer to 18%. The EAM produces a very high SR as the maximum SR of the EAM process component was 699 mm. However, for a fixed amount of current, the two processes can be compared. Literature reports that the SR/peak current of negative BEAM lies between 0.3 and 1.0. Almost 0.017 was the value for the positive beam BEAM. The SR/peak current for EDM also varied from 0.23 to 1.0.^{24 to 32}. Therefore, when the SRs of EDM and EAM process components are compared, it can be said that EAM and EDM produce the same amount of SR for unit current. Researchers have mostly used a water-based dielectric in EAM. Oil-based dielectrics are less effective at cooling than water-based dielectrics. Numerous studies have shown that EAM produces homogeneous and thin RCLs unlike EDM and thus has proven to be useful.^{7,14,16,19} Moreover, it further reduces machining and repair costs. Several studies have combined rotational and hydrodynamic fluid action to break the arc plasma, and none have used vibration (either tool or workpiece); most studies relied on the hydrodynamic action of the fluid.

DISTRIBUTION OF THE EAM'S PERCENTAGES

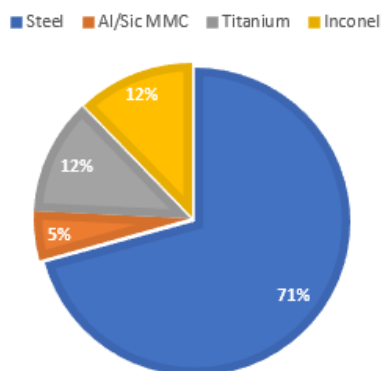


Figure 4: Distribution of the EAM's percentages depends on the material of the work item.

3. Future direction of research

Despite the fact that there is still much to learn, the scant amount of research on EAM shows that via theoretical and experimental studies, people have uncovered a vast array of potential applications. The majority of EAM research focuses on alloys made of steel. Figure 4 shows the percentage distribution of EAM performed on different materials. This suggests that there are many more materials with useful properties such as various metals and alloys, MMCs and superalloys. EAM needs to be explored. The only two properties most researchers have focused on are MRR and REWR. The geometric component is an important area to explore in addition to MRR and REWR. The mechanical properties of a machined part, such as its ultimate strength, flexural strength and shear strength, can be changed using EAM, a thermal energy-based technique. Additionally, this area needs to be explored. Although SR in EAM is very high, very few researchers have addressed this element of EAM quality. While EAM has shown that HABM is effective in interrupting plasma arcs, including RMABM can also make EAM function more efficient. Most researchers have used a water-based dielectric during EAM. During EAM, the effectiveness of different dielectrics can be investigated. In manufacturing industries, modeling and optimization are given a lot of weight. Only four researchers have developed the MRR, REWR, and SR, RSM models for EAM. Artificial Intelligence (AI) based modeling and optimization techniques such as ANN, Genetic Algorithms, Differential Evolution, Particle Swarm Optimization, Teacher Learning Based Optimization etc. can be very beneficial for various industries. AI-based modelling and optimization techniques were not used by any researchers throughout the EAM. This topic therefore requires extensive attention. The performance of UMPs can be greatly improved by combining UMPs with other conventional and non-UMP systems². Future studies should concentrate on this area as well.

3.1 Findings for Future Work

- Instead of alloy-based steel we can perform machining on metal matrix composites.
- Also, we can perform machining on hybrid metal matrix composites
- We can improve surface roughness as Material removal rate of electrical arc machining is higher as compared to electrical discharge machining.
- We prefer electrical arc machining for better material removal rate because electrical discharge machining having good surface roughness but its material removal rate is low.
- We can apply AI based modelling and optimization techniques to improve the performance of electrical arc machining process.

4. Conclusions

The complete analysis of the literature in the EAM is summarized as follows:

1. Low MRR machining efficiency is one of the primary issues with UMPs, which is resolved by the EAM. The largest MRR that has so far been achieved by scientists using EAM is 21,100 mm³/min. This is comparable to conventional machining methods and substantially greater than the majority of UMPs. Additionally, the TWR/REWR in the EAM is comparable to that in the EDM.
2. According to a thorough examination of the literature, polarity, peak current, and pulse-on time are the EAM's key determinants.
3. An extremely high SR is obtained from the EAM. The highest SR to date is 698 mm, according to published research. It is significantly higher than the SR found in the EDM. Sequential EDM and EAM can be used to produce parts with a high MRR and excellent surface polish.
4. The surface integrity achieved in the EAM is equivalent to that obtained in the EDM in terms of RCL and HAZ.
5. Steel has been the subject of the majority of EAM research. Other alloys have not been studied in any way. Additionally, relatively few researchers have looked into how the EAM can be used to machine superalloys and

metal-matrix composites.

6. Even though only a small number of EAM methods, including short electric arc machining, have been industrialized, other EAM procedures still have a sizable window of opportunity.
7. A few topics, including hybridization, modelling, and EAM optimization, have received little academic attention. It is necessary to investigate these regions.

5. Conflict of interest's statement

The author(s) did not disclose any potential conflicts of interest related to the study's research, authorship, or publishing.

6. Funding

The author(s) did not receive any financial support for the research, authorship, or publication of this paper.

References

1. Jain VK. *Advanced Machining Processes*. New Delhi, India: Allied Publishers, 2016.
2. Shrivastava PK and Dubey AK. EDM based-hybrid machining processes - a review. *Proc IMechE, Part B: J Engineering Manufacture* 2014; 228: 799–825.
3. Zhang M, Zhang Q, et al. Research on a single pulse discharge to discriminate EDM and EAM based on the plasma tunnel and crater geometry. *J Mater Process Technol* 2015; 219: 248–256.
4. Zhang M, Zhang Q, et al. Effects of flushing on electrical discharge machining and electro-arc machining. *Proc IMechE, Part B: J Engineering Manufacture* 2016; 230: 293–302.
5. Zhang R, Zhang Y, et al. Energy distribution and material removal of electric arc machining (EAM). *J Mater Process Technol* 2017; 242: 110–116.
6. Zhao W, Gu L, et al. A novel high efficiency electricalerosionprocess-blastingerosionarc machining. *Procedia CIRP* 2013; 6: 621–625.
7. Meshcheriakov G, Nosuienko V, et al. Physical and technological control of arc dimensional machining. *Annals CIRP* 1988; 37: 209–212.
8. Paul MA, Hodkinson NC and Aspinwall DK. Arcsawing of nickel based superalloys in aqueous electrolytes. *J Mater Process Technol* 1999; 92: 274–280.
9. Zhou J, Liang C, et al. Study on rules in material removal rate and surface quality of short electric arc machining process. *Adv Mater Res* 2008; 33: 1313–1318.
10. Crichton IM, McGeough JA, et al. Comparative studies of ECM, EDM and ECAM. *Precis Eng* 1981; 81: 155–160.
11. Wang F, Liu Y, et al. Machining performance of Inconel 718 using high current density electrical discharge milling. *Mater Manuf Process* 2013; 28: 1147–1152.
12. Gu L, Zhang F, et al. Investigation of hydrodynamic arc breaking mechanism in blasting erosion arc machining. *CIRP Ann: Manuf Technol* 2016; 65: 233–236.
13. Zhao W, Xu H, Gu L, et al. Influence of polarity on the performance of Blasting Erosion Arc Machining. *CIRP Ann: Manuf Technol* 2015; 64: 213–216.
14. Gu L, Chen J, et al. Blasting erosion arc machining of 20 vol.% SiC/Al metal matrix composites. *Int J Adv Manuf Technol* 2016; 87: 2775–2784.
15. Chen J, Gu L, et al. Study on blasting erosion arc machining of Ti-6Al-4V alloy. *Int J Adv Manuf Technol* 2016; 85: 2819–2829.
16. Xu H, Gu L, et al. Machining characteristics of nickel-based alloy with positive polarity blasting erosion arc machining. *Int J Adv Manuf Technol* 2015; 79: 937–947.
17. Shen Y, Liu Y and Sun W. High-efficient dry hybrid machining of EDM and arc machining. *Procedia CIRP* 2016; 42: 149–154.
18. Zhu G, Zhang Q, et al. Machining behaviors of short electrical arc milling with high frequency and high voltage pulses. *Int J Adv Manuf Technol* 2016; 90: 1067–1074.
19. Wang F, Liu Y, et al. Compound machining of titanium alloy by super high speed EDM milling and arc machining. *J Mater Process Technol* 2015; 214: 531–538.
20. Wang F, Liu Y, et al. Ultra-high-speed combined machining of electrical discharge machining and arc machining. *Proc IMechE, Part B: J Engineering Manufacture* 2014; 228: 663–672.
21. Zhou J, Geni M, et al. Analysis of the surface integrity machined by short electrical arc machining. *Key Eng Mater* 2011; 462: 1068–1074.
22. Zhou J, Xu Y, et al. Analysis and study on surface quality of workpiece of short electrical arc machining process. *Key Eng Mater* 2012; 522: 47–51.
23. Rao PN. *Manufacturing technology: metal cutting and machine tools*. New York: McGraw Hill Education, 2017.
24. Gaikwad V, Kumar V and Jatti S. Optimization of material removal rate during electrical discharge machining of cryo-treated NiTi alloys using Taguchi's method. *J King Saud Univ - Eng Sci* 2018; 30: 266–272.

25. Barenji V, Pourasli H and Khojastehnezhad VM. Electrical discharge machining of the AISI D6 tool steel: prediction and modeling of the material removal rate and tool wear ratio. *Precis Eng* 2016; 45:435–444.
26. Torres A, Puertas I and Luis J. Modelling of surface finish, electrode wear and material removal rate in electrical discharge machining of hard-to-machine alloys. *Precis Eng* 2015; 40:33–45.
27. Goyal A. Investigation of material removal rate and surface roughness during wire electrical discharge machining (WEDM) of Inconel 625 superalloy by cryogenic treated tool electrode. *J King Saud Univ – Eng Sci* 2017; 29:528–535.
28. Abidi MH, Al-Ahmari AM, et al. Multi-objective optimization of micro-electrical discharge machining of nickel-titanium-based shape memory alloy using MOGA-II. *Measurement* 2018; 125:336–349.
29. Kumar B, Kar BS and Potowari PK. Electric discharge machining of titanium grade 2 alloy and its parametric study. *Mater Today Proc* 2018; 5:5004–5011.
30. Jabbaripour B, Sadeghi MH, et al. Investigating the effects of EDM parameters on surface integrity, MRR and TWR in machining of Ti-6Al-4V. *Mach Sci Technol* 2012; 16:419–444.
31. Tang L and Du Y T. Multi-objective optimization of green electrical discharge machining Ti-6Al-4V in tap water via grey-taguchi method. *Mater Manuf Process* 2014; 29:507–513.
32. Singh G, Singh K, et al. Experimental studies on material removal rate, tool wear rate and surface properties of machined surface by powder mixed electrical discharge machining. *Mater Today Proc* 2017; 4:1065–1073.
33. Pandey S, Shrivastava P.K., Dangi S. Electrical Arc Machining: process capabilities and current research trends. Proceedings of the Mechanical Engineers, Part C: journal of Mechanical Engineering Science. Volume 233, Issue 15, pp 5190-5200, Sage Publication, 2019/8.
34. Phadke MS. *Quality engineering using robust design*. Prentice-Hall, Englewood Cliffs, NJ, 2023.
35. Gautam S, Singh P and Shrivastava PK. Modeling and Optimization of VEAM of 10% B4C/al Metal Matrix Composite using ANN-SCA Approach. *Engineering Research Express*; 2021, 3(3):1-13.